Introduction

This project is one component of trans-disciplinary research investigating the morphology of salt marshes in Oregon coastal estuaries as part of Oregon State University's (OSU) National Science Foundation (NSF) Research Traineeship (NRT) in risk and uncertainty quantification in marine sciences. We are particularly interested in how social and natural sources of sediment production into coastal estuaries have changed over time. Within the last century, Oregon coastal watersheds have been heavily impacted by human land use practices. Land use practices such as diking, logging, agriculture, and road building can greatly affect the sediment production of streams which in turn can affect the accumulation of sediment in estuaries on the coast. An important tool in investigating the environmental change within salt marshes is construction of lead-210 age-depth chronologies from salt marsh sediment cores. The focus of this Master's project is the statistical estimation of lead-210 age-depth chronologies using Bayesian methods.

Lead-210 is a radioactive isotope that is a daughter product in the uranium-238 decay series. It is naturally found in sediment and derives from uranium-238 within sediments and rocks (supported) or from the atmospheric fallout of radon-220 (unsupported). Radiometric analysis is used to analyze concentrations of excess (unsupported) lead-210 in sediments and construct lead-210 chronologies to track changes in sediment accumulation rates over time. Within sediment cores, supported lead-210 and unsupported lead-210 are indistinguishable. This leads to the necessity of placing assumptions and using mathematical models and proxy measurements to estimate lead-210 chronologies. In the measurement of lead-210 concentrations in laboratory settings, typically either alpha or gamma spectrometry is used. If gamma spectrometry is used then the concentration of lead-214 as the daughter product of radium-226 can be used as a proxy for supported lead-210. If alpha spectrometry is used then it is often assumed that the supported concentration of lead-210 down the length of a sediment core is constant. Furthermore, with use of alpha spectrometry researchers will often assume that the bottom measurements of unsupported lead-210 have reached close enough to zero that those bottom measurements can be used as proxies to the supported lead-210 concentration (Appleby (1998), Sanchez-Cabeza and Ruiz-Fernández (2012)). Different mathematical models have been developed to date lead-210 concentrations in sediment cores and construct age-depth chronologies. Due to its short half-life (22.3 years) the dating horizon for lead-210 chronologies is between 150 to 200 years. Accurate lead-210 age-depth chronologies are particularly useful for researchers interested in anthropocentric effects on ecological systems and environments within the last 200 years. In addition, sediment accumulation rates are also often of interest and can provide important information about ecological or environmental processes of a particular natural system.

While construction of accurate and reliable lead-210 chronologies is of great use to researchers, issues

with respect to measurement error and model error in lead-210 dating have not been extensively addressed through statistically modelling lead-210 age-depth chronologies. Recent work from Aquino-López et al. (2018) has extended Bayesian frameworks introduced in Blaauw and Christen (2011) for carbon-14 dating to lead-210 dating and produced the `Plum` package written in Python. In this project, we implement the Bayesian lead-210 model introduced by Aquino-López et al. (2018) in Stan (Stan Dev Team, 2018) using R (R Core Team, 2019) and propose the use of the Beta-Gamma autoregressive process of order 1 [BGAR(1)] from Lewis et al. (1989) as an alternative model of accumulation rates to that proposed by Aquino-López et al. (2018). We also extend the Bayesian lead-210 model framework to include multivariate t-likelihoods from Christen and Pérez (2009). We conduct a simulation study of the different Bayesian lead-210 models and highlight some of the work we have taken in applying the Bayesian lead-210 model to 15 salt marsh sediment cores from three different estuaries (Alsea Bay, Coquille, Nehalem Bay) along the Oregon coast to construct age-depth chronologies.

Approaches to Lead-210 Dating

Classic Approaches to Lead-210 Dating: the CRS Model

Let $P^U(x)$ be the concentration of unsupported lead-210 and $\rho(x)$ be the density of the core sample at depth x (Note that the International System of Units unit for radioactivity is the becquerel (Bq), concentrations of lead-210 are expressed in units of $\frac{Bq}{kg}$, density in $\frac{g}{cm^3}$, and depths in cm). Let $t(x)$ be an age-depth function which is the age of the core sample at depth x and assume that $t(x)$ is one-to-one. We are interested in inferring $t(x)$ from the core sample, although we do not directly observe $t(x)$.

Classic approaches to lead-210 dating rely upon mathematical models to convert concentrations of lead-210 into ages $t(x)$ along the depths of cores. These models place strong assumptions on how the supply of lead-210 accumulates through a given system which can lead to model misspecification. In addition, the classic mathematical models for lead-210 dating do not explicitly account for uncertainty in the measurement of lead-210 concentrations down the length of the core. Among the most common models applied to lead-210 dating is the constant rate of supply (CRS) model (Appleby and Oldfield, 1978).

In the CRS model it is assumed that the rate at which lead-210 is supplied to the surface is constant with respect to time. That is the initial concentration of unsupported lead-210 $P_0^U(t(x))$ and the dry mass sedimentation rate $r(t(x))$ (as expressed as a function of time corresponding to depth x) are balanced by a

constant Φ, known as the initial supply of lead-210 (measured in $\frac{Bq}{m^2 yr}$):

$$P_0^U(t(x))r(t(x)) = \Phi.$$

The dry mass sedimentation rate is the rate at which sediment accumulates weighted by density:

$$r(t(x)) = \rho(x)\frac{dx(t)}{dt},$$

where $x(t) = t^{-1}(x)$ and $\frac{dx(t)}{dt} = \left(\frac{dt(x)}{dx}\right)^{-1}$ is the rate at which sediment accumulates with respect to time. To find the unsupported concentration of lead-210, $P^U(x)$, at depth x, using the radioactive decay equation gives

$$P^U(x) = P_0^U(t(x))e^{-\lambda t(x)}$$

where $\lambda = 0.03114$ is the decay constant of lead-210.

The unsupported activity of lead-210 over a core section (a, b) is the integral of the unsupported concentration of lead-210 weighted by the density of the core section:

$$A^U(a,b) = \int_a^b \rho(x)P^U(x)dx = \frac{\Phi}{\lambda}\left(e^{-\lambda t(a)} - e^{-\lambda t(b)}\right).$$

Denote the unsupported activity below depth x as

$$A^U(x) = \int_x^\infty \rho(x)P^U(x)dx = \frac{\Phi}{\lambda}e^{-\lambda t(x)}.$$

Note then that the unsupported activity of the whole core can be written as $A^U(0) = \int_0^\infty \rho(x)P^U(x)dx = \frac{\Phi}{\lambda}$ such that we can write $A^U(x) = A^U(0)e^{-\lambda t(x)}$. Based on this equation, the CRS model provides the following equation as the age-depth function:

$$t(x) = \frac{1}{\lambda}\log\left(\frac{A(0)}{A(x)}\right),$$

where $\log(\cdot)$ is the natural logarithm. As Appleby (1998), Sanchez-Cabeza and Ruiz-Fernández (2012), and Aquino-López et al. (2018) note, one serious shortcoming with the CRS model is that it relies on the assumption that the unsupported activity for the entire core, $A(0)$, can be reliably measured. If the total activity of lead-210 does not reach background levels by the end of the core, then the measurement of $A(0)$ will be biased and the subsequent ages will be miscalibrated (Appleby, 1998). Unfortunately, the instruments used to measure lead-210 concentrations often have detection limits so some form extrapolation is necessary in using the CRS method. However, use of extrapolation comes with its own set of assumptions

and the errors associated with extrapolating are not accounted for in a subsequent CRS calculation. An additional issue with the CRS model is that because $A(x)$ will decay exponentially as the depth increases, $t(x)$ will artificially increase in such a way that does not accurately reflect changes in the underlying sediment accumulation rates.

Bayesian Model for Lead-210 Dating

Success with applying Bayesian frameworks to carbon-14 dating (Blaauw and Christen, 2011) and implementation through the `Bacon` package in `R` has lead researchers to apply a Bayesian framework to lead-210 dating. The benefit of the Bayesian framework is that the uncertainty in ages and other parameters of the mathematical models are accounted for explicitly in the statistical set-up of the lead-210 dating model. In addition, the Bayesian lead-210 dating model does not use the ratio $\frac{A(0)}{A(x)}$ and so avoids the problem of artificially old dates or the need to measure the activity of the whole core accurately. The Bayesian lead-210 model makes use of deeper sections of the core compared to the CRS model, allowing for longer chronologies to be constructed. An alternative to the Bayesian approach is to use Monte Carlo error propagation methods as discussed in Binford (1990) and Sanchez-Cabeza et al. (2014) in conjunction with the CRS model.

Lead-210 Activity

Aquino-López et al. (2018) set up their Bayesian Lead-210 dating model as follows. Let p_i denote the concentration of lead-210 measured in a sample taken from core section $(x_i - \delta, x_i)$ where there are $i = 1, \ldots, N$ core section depths x_i and δ is the constant height of each core section. We assume that $p_i | P_i^T \sim N(P_i^T, \sigma_i^2)$ where P_i^T is the unknown total concentration of the ith core section and σ_i^2 is the laboratory reported variance. Since the concentration p_i of each core section is measured independently of the others we assume the concentration p_i of lead-210 between different core sections are independent conditional on the unknown total concentration P_i^T of each section.

The total concentration of lead-210, P_i^T, for each section is the sum of the unknown supported and unsupported lead-210 concentrations in that section: $P_i^T = P_i^U + P_i^S$, where P_i^U is the unsupported lead-210 concentration and P_i^S is the supported lead-210 concentration for the ith core section. In general, an assumption of constant supported concentration is used in the model. That is, for all core sections $i = 1, \ldots, N$, $P_i^S = P^S$ where P^S is the unknown constant supported concentration. Using the constant supported concentration assumption reduces model complexity by reducing number of unknown parameters. Aquino-Lopez argues that it is preferable to use constant supported concentration unless it can be shown the the assumption does not hold. This may particularly be the case if concentrations of lead-214 have not

been measured in each core section, since in these cases the supported concentration is estimated in the lower depths of the core sample where it is assumed that the unsupported activity has reached background levels. However, if lead-214 measurements are available, then it may be preferable to use non-constant supported concentration (Appleby, 1998), particularly if the physical system the sediment core is taken from indicates that constant supported concentration assumption is not valid. For the purpose of this project, when considering the framework of the Bayesian lead-210 model, we will consider P_i^S to be non-constant across sections but constant within each section. That said, any of the following will still be valid if the supported concentration in the core is constant.

The lead-210 activity in the ith core section is given by

$$A_i^T = \int_{x_i-\delta}^{x_i} \rho_i(z) P_i^T(z) dz = \int_{x_i-\delta}^{x_i} \rho_i(z) P_i^U(z) dz + \int_{x_i-\delta}^{x_i} \rho_i(z) P_i^S(z) dz$$

where $\rho_i(z)$ is the density at depth z of the ith core section, $P_i^U(z)$ is the unsupported concentration at depth z, and $P_i^S(z)$ is the supported concentration at depth z. To obtain the unsupported activity in the ith core section, Aquino-López et al. (2018) assumes a constant rate of supply and integrating over unsupported concentration weighted by density gives

$$A_i^U = \int_{x_i-\delta}^{x_i} \rho_i(z) P_i^U(z) dz = \int_{t(x_i-\delta)}^{t(x_i)} \Phi e^{-\lambda y} dy = \frac{\Phi}{\lambda} \left(e^{-\lambda t(x_i-\delta)} - e^{\lambda t(x_i)} \right),$$

where Φ is the initial supply of the lead-210 and $t(z)$ is the age of the sample at depth z. Next note that the density of the ith core section is given by $\rho_i = \int_{x_i-\delta}^{x_i} \rho_i(z) dz$. As we assume that P_i^S is constant in the ith core section but varies between core sections, the supported activity of the ith core section is given by

$$A_i^S = \int_{x_i-\delta}^{x_i} \rho_i(z) P_i^S dz = \rho_i P_i^S.$$

Define the measured activity of the ith core section by

$$y_i = \int_{x_i-\delta}^{x_i} \rho_i(z) p_i dz = \rho_i p_i.$$

The distribution of y_i is given by

$$y_i | P_i^S, \Phi, \tilde{t} \sim N \left(A_i^S + \frac{\Phi}{\lambda} \left(e^{-\lambda t(x_i-\delta)} - e^{-\lambda t(x_i)} \right), (\sigma_i^2 \rho_i^2) \right),$$

where $\tilde{t} = (t(x_0), t(x_1), \ldots, t(x_N))$ and $x_0 = x_1 - \delta$. It is important to note that the age depth function $\tilde{t}$ is

treated as a latent variable in the model. The initial supply of sediment Φ and the supported concentration P_i^S are physically interpretable parameters within the model and may not be of primary concern for researchers.

Age-Depth Function

In their approach towards constructing the age-depth function, Aquino-López et al. (2018) rely on the Bacon age-depth function developed by Blaauw and Christen (2011). The age-depth function from Bacon involves a series of linear interpolations of the form

$$G(x, m) = \sum_{j=1}^{k} m_j \delta + m_{k+1}(x - x_k)$$

where $x_k \leq x \leq x_{k+1}$, $k < N$, and $m = (m_1, \ldots, m_N)$ are the sediment accumulation rates (yr/cm) for each core section. The age-depth function assumes that the rate of sediment accumulation within a core section increases linearly while allowing for the rates to vary between core sections.

As accumulation rates must generally be positive, it is necessary to find a distribution for m. Blaauw and Christen (2011) propose the use of a gamma autoregressive model. For $j = 1, \ldots, N$, let $\alpha_j \overset{iid}{\sim} Gamma(a_\alpha, b_\alpha)$ where a_α and b_α represent parameter values summarising prior information available on accumulation rates. Set $m_N = \alpha_N$ and for $j = 1, \ldots, N-1$, let

$$m_j = \omega m_{j+1} + (1 - \omega)\alpha_j,$$

where $\omega \in [0, 1]$. The accumulation rate m_j is a weighted average between the accumulation rate m_{j+1} of the previous core section and i.i.d. Gamma-distributed noise. The weighting parameter ω represents the "memory" or dependence of the accumulation rates along the core when modeled as an autoregressive process (where $\omega = 0$ indicates independence and $\omega = 1$ represents a fixed process). Blaauw and Christen (2011) state that ω functions as a smoothing parameter for the autoregressive process and suggests a $Beta(a_\omega, b_\omega)$ as a prior distribution for ω. In addition, given ω, a_α, b_α, we can write $m_j = \omega m_{j+1} + \beta_j$, where $\beta_j \sim Gamma\left(a_\alpha, b_\alpha/(1-\omega)\right)$. Blaauw and Christen (2011) interpret the Gamma autoregressive model in the context of the work of Barndorff-Nielsen and Shepard (2003) where the process can be seen as the discrete approximation of the continuous time Ornstein-Uhlenbeck process with gamma innovations.

As an alternative we propose the use of the Beta-Gamma autoregressive model of order 1 or BGAR(1) process first introduced by Hugus (1982) and described by Lewis et al. (1989). With the BGAR(1) process, we can construct an autoregressive process that is marginally $Gamma(a_\alpha, b_\alpha)$ distributed and where the dependency structure depends on a single parameter ψ. Let $\psi \in (0, 1)$ and $\bar{\psi} = 1 - \psi$. Once again let

$m_1, \ldots, m_N$ denote the accumulation rates for each core section. Let $\omega_1, \ldots, \omega_{N-1} \overset{iid}{\sim} Beta(a_\alpha \psi, a_\alpha \overline{\psi})$, $\alpha_1, \ldots, \alpha_{N-1} \overset{iid}{\sim} Gamma(a_\alpha \overline{\psi}, b_\alpha)$ and $m_N = \alpha_N \sim Gamma(a_\alpha, b_\alpha)$ and assume that ω_j's, α_i's, and m_N are mutually independent. Then for $j = 1, \ldots, N-1$, set

$$m_j = \omega_j m_{j+1} + \alpha_j.$$

Based on the Beta-Gamma transformation described by Lewis et al. (1989), it can be shown that marginally the m_j's are $Gamma(a_\alpha, b_\alpha)$ distributed. In addition, Lewis et al. (1989) show that for $k = 0, \pm 1, \pm 2, \ldots$, that $Corr(m_j, m_{j+k}) = \psi^{|k|}$ such that the m_j form a weakly (2nd order) stationary process. Given that $\psi \in (0, 1)$, we use a $Beta(a_\psi, b_\psi)$ prior distribution for the dependence parameter ψ, although it is certainly possible to use a reference prior. One possible benefit of considering the BGAR(1) process in modelling the accumulation rates is that it provides greater flexibility than the Gamma autoregressive process proposed by Blaauw and Christen (2011). Each ω_j functions as a weighting factor for each core section while still preserving the autoregressive dependence structure between accumulation rates. One tradeoff with the BGAR(1) process is that it is more complex and increases the dimension of the parameter spaces at the cost of increased flexibility. In addition, the choice of the prior distribution for ψ takes a greater role in the tuning of the model given the ω_j's are sampled from a Beta distribution depending on the values of ψ. This added hierarchical structure along with the increase in dimensionality may make it considerably more difficult for an MCMC sampler to efficiently explore the surface of the log-likelihood function of the model. However, the BGAR(1) process can be generalized to moving average and ARMA-type structures based on the work of Lewis et al. (1989) which could be of potential use if a sediment accumulation process warrants a more complex dependency structure.

Normal Likelihood

Supported activity is estimated either from measurements of lead-214 or from assuming that the bottom sections of the core sample have reached background. Measurements of supported concentration are denoted as p_i^S for $i = 1, \ldots, n_S$ where n_S is the number of measurements of supported concentration. The supported activity is then defined to be $y_i^S = \rho_i p_i^S$. Combining the age-depth function from above with the distribution of the measured total and supported activity provides a log-likelihood function of the form

$$\ell(\tilde{y}, \tilde{y}^S | m, \omega, \Phi, \tilde{P}^S) \propto -\sum_{i=1}^{N} \frac{(y_i - (A_i^S + \frac{\Phi}{\lambda}(e^{-\lambda G(x_{i-1} m)} - e^{-\lambda G(x_i, m)})))^2}{2\rho_i^2 \sigma_i^2} - \sum_{j=1}^{n_S} \frac{(y_j^S - A_i^S)^2}{2\rho_j^2 \sigma_j^2}$$

where $\tilde{y} = (y_1, \ldots, y_N)$, $\tilde{y}^S = (y_1^S, \ldots, y_{m_S}^S)$, and $\tilde{P}^S = (P_1^S, \ldots, P_{m_s}^S)$.

Prior Distributions

Aquino-López et al. (2018) suggest specific priors for each parameter within the model. For example, they suggest a $Gamma(a_\Phi, b_\Phi)$ for the initial supply Φ such that $E[\Phi] = 50$. For the supported lead-210 P^S, Aquino-López et al. (2018) suggest as a prior that $P^S \sim Gamma(a_S, b_S)$ where a_S and b_S are chosen such that $E[P^S] = 20$. While they suggest for the Gamma priors, a shape parameter of 2, we tend to set the shape parameter equal to 1.

With respect to the Gamma autoregressive process, for ω, we use a $Beta(a_\omega, b_\omega)$ prior distribution. We tried setting $a_\omega = b_\omega = 0.5$ for ω (corresponding to the Jeffrey's prior for the Beta distribution). However, this can lead to the posterior distribution of ω focusing too much to the upper tail near 1. Rather, we find that choosing a_ω and b_ω such that $a_\omega < b_\omega$ and $E[\omega] \approx 0.5$ (for example, setting $a_\omega = 1.1$ and $b_\omega = 1.2$ tends to provide agreeable results for most sediment cores. In our experience, the prior distributions for Φ and P^S do not have a considerable effect on the convergence of the MCMC or validity of the Bayesian lead-210 model as compared to the prior distribution for the i.i.d. $Gamma(a_\alpha, b_\alpha)$-distributed errors $\alpha_1, \ldots, \alpha_N$. One strategy we have found effective is to set the shape parameter $a_\alpha = 1$ and have the rate parameter b_α be equal to the inverse of the mean sediment accumulation rate obtained from the CRS model. This choice of prior makes it so that $E[m_N]$ is equal to the mean sediment accumulation rate from the CRS model. While this is a fairly informative prior, it is likely a reasonable choice since the mean sediment accumulation rate from the CRS model is likely in the neighborhood of the true sediment accumulation rate. Furthermore, the parameter space for the Bayesian lead-210 model is high-dimensional, the model is overparameterized, and the sample size is typically low (on the order of 10 to 30 core sections per sediment core). Using a relatively informative prior for the accumulation rate is improtant so that the MCMC sampler does not get stuck exploring less plasuible areas on the surface of the log-likelihood function.

Setting priors for the BGAR(1) process is more difficult given the structure of the model and the fact that using the BGAR(1) process to model the sediment accumulation rates can effectively double the number of unknown parameters in the model. We would still want to set the prior for m_N such that $E[m_N]$ is equal to the CRS accumulation rate. However, greater care must be taken in choosing the shape parameter a_α considering that $\omega_1, \ldots, \omega_{N-1} \overset{iid}{\sim} Beta(a_\alpha\psi, a_\alpha\overline{\psi})$ where $\psi \sim Beta(a_\psi, b_\psi)$. Because $\psi \in (0, 1)$, if we set $a_\alpha = 1$, then the posterior distributions for the ω_i will typically be heavily skewed near 1. So likely it is necessary to set $a_\alpha > 1$. One possible strategy is to set a_ψ and b_ψ so that ψ is tightly dispersed around some reasonable value in $(0, 1)$. Doing so may ensure that $\omega_1, \ldots, \omega_{N-1}$ are not drawn from near the border of $(0, 1)$. Given that the geometry of the parameter space of the BGAR(1) Bayesian lead-210 model is high-dimensional, complicated, and exhibits hierarchical dependencies, it may also be worthwhile to pursue

alternative parameterizations of the model so that the the geometry is not as complicated for the MCMC sampler to traverse.

Multivariate t-likelihood

In order to account for measurement error and model robustness to non-normality, it is possible to use a multivariate t-likelihood instead of the Normal likelihood introduced above. Christen and Pérez (2009) introduce a robust t-likelihood based model for radiocarbon data which we adapt for use in the lead-210 model.

In particular, let $\Theta = (m, \omega, \Phi, \tilde{P}^S)$ denote the parameters of the model. Consider $y = (\tilde{y}^t, (\tilde{y}^S)^t)^t$ and assume that $\tilde{y}$ and $\tilde{y}^S$ are independent. The Normal likelihood is given by

$$L(\Theta|\tilde{y}, \tilde{y}^S) \propto \left(\prod_{j=1}^{N} \frac{1}{\sqrt{\rho_j^2 \sigma_j^2}} \exp\left(-\frac{(y_j - \mu_j(\Theta))^2}{2\rho_j^2\sigma_j^2} \right) \right) \cdot \left(\prod_{k=1}^{m_S} \frac{1}{\sqrt{\rho_k^2 \sigma_k^2}} \exp\left(-\frac{(y_k^S - \mu_k^S(\Theta))^2}{2\rho_k^2\sigma_k^2} \right) \right)$$

where $\mu_j(\Theta) = A_i^S + \frac{\Phi}{\lambda}\left(e^{-\lambda G(x_{i-1}m)} - e^{-\lambda G(x_i, m)}\right)$ and $\mu_k^S(\Theta) = A_k^S$. In other words, for $j = 1, \ldots, N$, $y_j \sim N\left(\mu_j(\Theta), \rho_j^2\sigma_j^2\right)$ for observations related to the total activity and for $k = 1, \ldots, m_S$, $y_k^S \sim N\left(\mu_k^S(\Theta), \rho_k^2\sigma_k^2\right)$ for observations related to the supported activity with the y_j's and y_K's independent. Let $n = N + m_S$ and for $j = 1, \ldots, N$, we let y_j correspond to the total activity and $\mu_j(\Theta) = A_i^S + \frac{\Phi}{\lambda}(e^{-\lambda G(x_{i-1}m)} - e^{-\lambda G(x_i, m)})$ while for $j = N+1, \ldots, N+m_S = n$, we let $y_j = y_{j-N}^S$ and $\mu_j(\Theta) = \mu_{j-N}^S(\Theta)$ corresponding to the $j - N$th supported activity measurement.

With the Normal likelihood, we assume that the variance σ_j^2 is known exactly and given by the reporting laboratory. We may however suppose that the true variability of the measured activity to be dependent on a strictly-positive unknown variance multiplier ξ. In this case for $j = 1, \ldots, n$, we then have

$$y_j \sim N(\mu_j(\Theta), \xi\rho_j^2\sigma_j^2)$$

and the joint-likelihood with respect to (Θ, ξ) is written as

$$L(\Theta, \xi|y) \propto \xi^{-\frac{n}{2}} \prod_{j=1}^{n} \frac{1}{\sqrt{\rho_j^2\sigma_j^2}} \exp\left(-\frac{1}{2\xi\rho_j^2\sigma_j^2}(y_j - \mu_j(\Theta))^2 \right).$$

It may also be possible to consider unknown variance multipliers ξ_1 and ξ_2 where ξ_1 corresponds to the measurement of the total activity while ξ_2 corresponds to the measurement of the supported activity. This may reflect the fact that measurements of supported activity in Lead-210 can be made through measurement of lead-214 in the core sections.

Assume that the prior distribution for ξ is an inverse gamma distribution with shape parameter a and scale parameter b since ξ essentially models an unknown Normal variance. Christen and Perez note that given the prior for ξ does not depend on Θ. While prior values for a and b are necessary, Christen and Perez suggest that as default values $a = 3$ and $b = 4$ should be considered as this places a stronger probability on the reported standard error being underestimated by a factor between 1 and 2. For sake of simplicity, in the implementation of the following multivariate t-likelihood in the Bayesian lead-210, we chose to follow Christen and Perez's suggested values for the parameters of the prior of ξ to be $a = 3$ and $b = 4$, although we suggest that other choices for the parameters at least be explored for different applications.

For use in the Bayesian lead-210 model, note that ξ is a nuisance parameter while researchers are typically interested in Θ. The natural approach to get rid of ξ is to marginalize the joint likelihood (Θ, ξ) by integrating out ξ. In particular, note that the likelihood with respect to Θ can be written as

$$\pi(y|\Theta) = \int \pi(y, \xi|\Theta) d\xi = \int \pi(y|\Theta, \xi)\pi(\xi) d\xi$$

where $\pi(y|\Theta, \xi) = L(\Theta, \xi|y)$ and $\pi(\xi)$ is the prior distribution of ξ. Using the inverse-gamma prior for ξ and noting that the $y_j|\Theta, \xi \sim N(\mu_j(\Theta), \xi\rho_j^2\sigma_j^2)$ are independent conditional on Θ and ξ, the likelihood with respect to Θ is then given by

$$\begin{aligned}
L(\Theta|y) &\propto \int_0^\infty \prod_{j=1}^n \pi(y_j|\Theta, \xi)\pi(\xi) d\xi \\
&= \int_0^\infty \xi^{-\frac{n}{2}} \prod_{j=1}^n \frac{1}{\sqrt{\rho_j^2\sigma_j^2}} \exp\left(-\frac{1}{2\xi\rho_j^2\sigma_j^2}(y_j - \mu_j(\Theta))^2\right) \xi^{-(a+1)} \exp\left(-\frac{b}{\xi}\right) d\xi \\
&\propto \left(b + \sum_{j=1}^n \frac{(y_j - \mu_j(\Theta))^2}{2\rho_j^2\sigma_j^2}\right)^{-\frac{2a+n}{2}} \\
&\propto \left(1 + \frac{1}{2a}\sum_{j=1}^n \frac{(y_j - \mu_j(\Theta))^2}{2\rho_j^2\sigma_j^2 b/a}\right)^{-\frac{2a+n}{2}} \\
&= \left(1 + \frac{1}{2a}(y - \tilde{\mu}(\Theta))^t \Sigma^{-1}(y - \tilde{\mu}(\Theta))\right)^{-\frac{2a+n}{2}},
\end{aligned}$$

where $\tilde{\mu}(\Theta) = (\mu_1(\Theta), \ldots, \mu_n(\Theta))^t$ and $\Sigma = \text{diag}(\rho_1^2\sigma_1^2, \ldots, \rho_n^2\sigma_n^2) \cdot \frac{b}{a}$. The full calculation can be completed using the appropriate change of variable in the integral. With the last line, the likelihood with respect to Θ is proportional to the kernel of a multivariate t-distribution with location parameter $\tilde{\mu}(\Theta)$, covariance matrix Σ, and $2a$ degrees of freedom. Hence once ξ is marginalized, we have $y|\Theta \sim t(\tilde{\mu}(\Theta), \Sigma, 2a)$. In general, issues of non-normality or measurement error may be a larger problem with carbon-14 dating due to the variety

of measuring techniques used in that application compared to in lead-210 dating. In addition, laboratories often carefully calibrate instruments used to measure lead-210 concentrations to minimize instrumental drift. Non-normality may not be a large concern with lead-210 in choosing to use the multivariate t-likelihood. On the other hand, the relatively small sample size ($N = 10$ to 30) of lead-210 core measurements may mean that the fatter tails of the t-distribution better capture the uncertainty in the data.

Implementation

While the `Plum` package developed by Aquino-López et al. (2018). implements the Bayesian lead-210 model, it is written in Python. We chose to implement the Bayesian lead-210 models in Stan with control scripts handled in R via the `RStan` package (Stan Dev Team, 2018). In their implementation, Aquino-López et al. (2018) utilize a self-adjusting MCMC algorithm known as the t-walk developed by Christen and Fox (2010). However, we felt that there were advantages to coding the model in Stan such as the efficiency of the No U-turn Sampler (NUTS) and the general Hamiltonian Monte Carlo set-up utilized in Stan. While the model coded in Stan requires some exploration of prior choices to achieve representative posterior distributions for ages and accumulation rates, it is relatively easy to tune and provides built in convergence diagnostics to aid with trouble shooting of MCMC chains.

Simulation

To assess the accuracy and precision of the different lead-210 models, we utilized the simulation set-up from Aquino-López et al. (2018). Utilizing the constant rate of supply assumption, the initial supply is set at $\Phi = 150$ and supported supply at $P^S = 20$. The age-depth function is defined to be $t(x) = x^2/3 + x/2$ and we used the density function $\rho(x)$, initial concentration $P_0(x)$, and unsupported concentration function $P^U(x)$ found in Aquino-López et al. (2018). The concentration for the ith sample is given by $P_i = P^S(b-a) + \int_a^b P^U(x)dx$ where a and b are the top and bottom depths of the sample. We added Gaussian noise $\epsilon_i \sim N(0, \sigma_i^2)$ to P_i, where the standard deviations σ_i are provided in Table 1 of the appendix. To simulate the measurements of lead-214, we drew supported concentration measurements $p_i^S \sim N(20, \sigma_i^2)$ for $i = 1, \ldots, 30$.

We chose to test the performance of the models using the Normal likelihood, t-likelihood, BGAR(1) with Normal likelihood, and BGAR(1) with t-likelihood in two different scenarios using this dataset. In the first scenario we do not use the simulated lead-214 measurements and instead we use the bottom 3 measurements of simulated total concentration to estimate the supported concentration P^S in the model. This corresponds to situations where alpha spectrometry is used to measure lead-210 concentrations in sediment cores. In the second scenario, we use the simulated lead-214 concentration measurements to estimate the supported

concentration P^S in the model. This corresponds to situations where gamma spectrometry is used to measure lead-210 concentrations which also allows measurement of lead-214 concentrations.

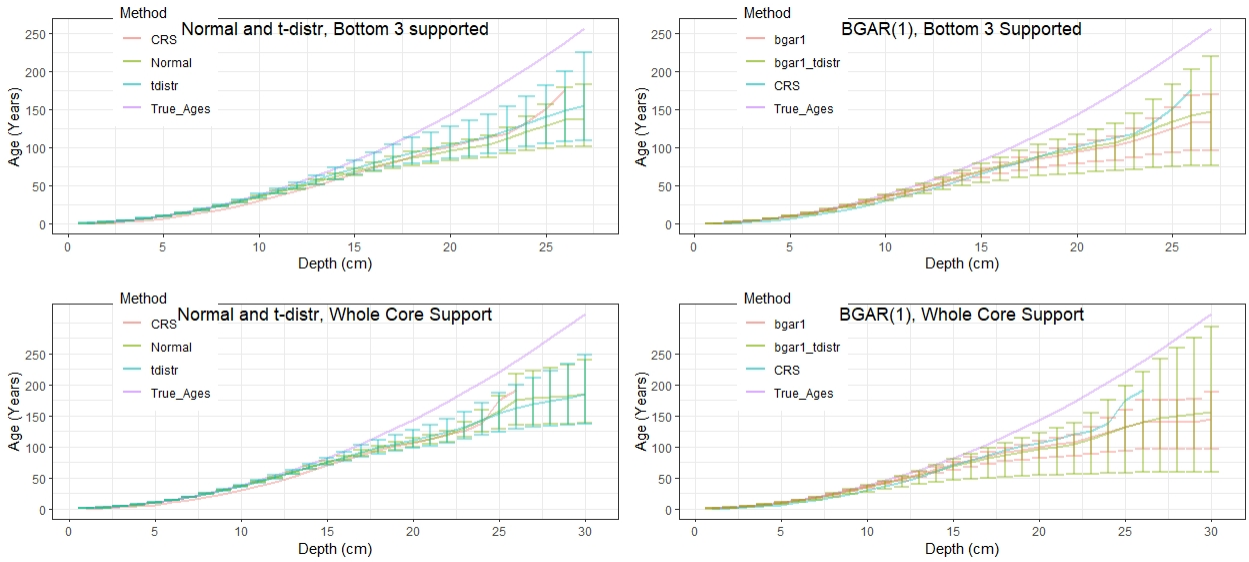

Figure 1: Mean posterior age-depth functions with 95% credible intervals for simulated dataset

Using the Stan code we used to implement the Bayesian lead-210 models, we ran MCMC samplers of the 4 different models across the two scenarios. We chose to run each model across 4 chains for 200,000 iterations each, of which 100,000 iterations were used as a burn-in period. The adapt_control argument in the Stan control script was set to 0.99 to decrease the step-size taken at each iteration of the sampler. While this decreased the speed at which the MCMC algorithm ran, this ensured that there were no divergent transitions after the burn-in period and was necessary given that the Bayesian lead-210 likelihoods are likely multimodal and geometrically complex. On the other hand, with some of the lead-210 models the small step size lead to issues with the efficiency of the MCMC sampler. We chose to set informative priors for the initial supply Φ, supported activity P^S, and Gamma noise to test a best case scenario with respect to our knowledge of the simulated sediment core. With real-world sediment cores, we usually have some scientific knowledge guiding how we set the priors. Once simulations were run, we compared the posterior age-depth function with both the true age-depth function and the ages coming from the CRS model. The Normal and t-likelihood lead-210 models did not have any exceptional issues with respect to model convergence in either scenario. With the BGAR(1) models using the Normal and t-likelihood there were significant issues with respect to the efficiency the algorithm. There were divergent transitions for the BGAR(1) models using the Normal likelihoods for both scenarios but no divergent transitions for the BGAR(1) models using the t-likelihoods in either scenario. R-hat statistics for the BGAR(1) models were in the range of 1.2 to 1.8 for

some parameters while the n_{eff} was quite low across all four BGAR(1) models we fit, indicating difficulty with the convergence of the MCMC with these specific models.

In Figure 1, we plot the posterior age-depth functions for the 4 models across the two scenarios along with the ages from the CRS model and the true age-depth function and include the 95% credible intervals for each model. To the left are the Normal and t-likelihoods using the Gamma autoregressive process from Aquino-López et al. (2018) while to the right are the Normal and t-likelihoods using the BGAR(1) process we propose. The top panels use the bottom 3 samples of the simulated total concentration measurements to estimate the supported activity while the bottom panels use the simulated supported concentration measurements to estimate the supported activity. One thing to note is that none of the methods are able to accurately capture the true age-depth function. This is likely due to the physical constraints placed on the models by the fact that the half-life of lead-210 is relatively short (22.3 years) and thus has a dating horizon of around 150-200 years depending on the initial supply Φ. However, we would like to note that the Bayesian lead-210 models can estimate ages for deeper core sections than the CRS model. Furthermore, the Bayesian lead-210 models do not suffer from the artificial sharp increase in ages near the bottom of the core that the CRS model does (Appleby, 1998).

Based on these simulation runs, it appears that it is advantageous to implement multivariate t-likelihoods with Bayesian lead-210 models. Some of the models utilizing Normal likelihoods did not fully include the CRS model within the 95% credible intervals in either scenario. On the other hand, utilizing t-likelihoods with or without using the BGAR(1) process led to more accurate posterior age-depth functions which fully included the CRS model within the 95% credible interval. The 95% credible intervals for the t-likelihood lead-210 models are generally wider near the bottom of the core compared to models using Normal likelihoods. Despite the wider intervals, it appears that the t-likelihood lead-210 models are outperforming Normal likelihood lead-210 models with respect to estimating the age at each depth and appropriately accounting for the uncertainty present in the simulation data.

As noted, there were some serious issues with respect to the convergence of lead-210 models utilizing the BGAR(1) process. This is likely due to how the choice of prior distributions for the dependence parameter ψ and the bottom depth Gamma error α_N affect how for $j = 1, \ldots, N-1$ both the ω_j and the α_j are drawn from their prior distributions. Despite these issues, the BGAR(1) models performed relatively similarly to the non-BGAR(1) models, although in comparison the BGAR(1) models appear to underestimate the true ages. The upper bound posterior ages of the 95% credible intervals for the BGAR(1) model using the t-likelihood were closest to the true ages. This indicates some of the potential in using the BGAR(1) process to model the sediment accumulation rates in Bayesian lead-210 models.

Application

As an application, we ran the Bayesian lead-210 model on the ABOR1309_02 salt marsh sediment core from Alsea Bay on the Oregon Coast collected and analyzed by Peck et al. (2019). We ran both the Normal and t-likelihood lead-210 models utilizing the Gamma autoregressive process from Aquino-López et al. (2018) in Stan for 200,000 iterations across four chains. Here we see that the Normal and t-likelihoods provide similar posterior age-depth functions and 95% credible intervals while both containing the ages from the CRS model. In addition, neither of the Bayesian lead-210 models ran here appear to suffer from miscalibration as seriously as the CRS model.

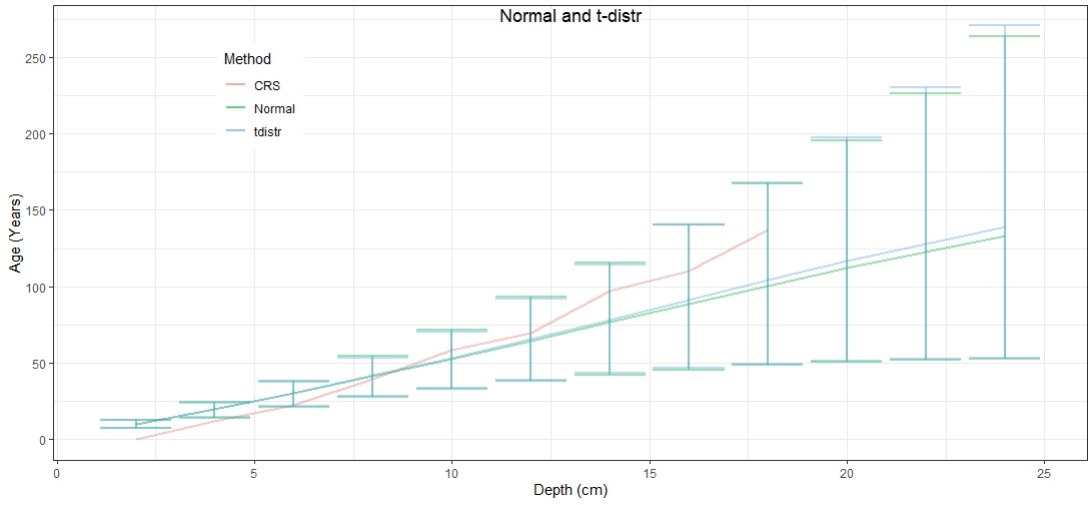

Figure 2: Mean posterior age-depth functions with 95% credible intervals for the ABOR1309_02 Alsea sediment core

Discussion

In this project we introduced several extensions to the Bayesian lead-210 model initially developed by Aquino-López et al. (2018). Through both simulation and application, it appears that there is a benefit to utilizing t-likelihoods rather than Normal likelihoods with lead-210 models although this should be tested further in more simulations under more realistic conditions. The BGAR(1) process of Lewis et al. (1989) which we introduced to model the sediment accumulation rates showed some promise. It is a more flexible process than the Gamma autoregressive process used by Aquino-López et al. (2018) and may be useful for modelling a wider range of sediment accumulation scenarios within a sediment core. However, for the BGAR(1) process to be useful in the Bayesian lead-210 modelling framework, the poor convergence and other diagnostic issues

with the MCMC need to be addressed. While further exploration of the prior distribution choice should be considered, it may be most fruitful to focus future efforts on finding a more tractable reparameterization of the BGAR(1) process. A good reparameterization may simplify some of the selection of the prior distributions and improve the convergence of the MCMC sampler. As Aquino-López et al. (2018) mention, it is possible to use the Bayesian lead-210 model to combine lead-210, carbon-14, and cesium-137 sediment core data to construct potentially more robust age-depth chronologies. In addition, further simulations are necessary to determine the properties of various formulations of the Bayesian lead-210 model under varying conditions including with unusual age-depth functions, non-constant support, systematic measurement error, and missing data. There are many advantages and some disadvantages to the Bayesian lead-210 model compared to the CRS model, and further work is needed to fully understand both the advantages and disadvantages of using the Bayesian lead-210 model to construct age-depth chronologies.

References

Appleby, P.G. (1998), "Dating recent sediments by Pb-210: Problems and solutions," *Proc 2nd NKS/EKO-1 Seminar, Helinski, 2-4 April 1997 STUK, Helsinki,* pp. 7-24.

Appleby, P., and Oldfield, F. (1978), "The calculation of lead-210 dates assuming a constant rate of supply of unsupported 210Pb to the sediment," *Catena*, 5(1), 1-8.

Aquino-López, M.A., Blaauw, M., Christen, J.A., and Sanderson, N.K. (2018), "Bayesian Analysis of ^{210}Pb Dating," *Journal of Agricultural, Biological and Environmental Statistics,* 23, 317-333. https://doi.org/10/1007/s13253-018-328-7.

Barndorff-Nielsen, O.E. and Shephard, N. (2003), "Non-Gaussian Ornstein-Uhlenbeck-based models and some of their uses in financial economics (with discussion)." *Journal of the Royal Statistical Society, Series B,* 63: 167-241.

Binford, M.W. (1990), "Calculation and uncertainty analysis of ^{210}Pb dates for PIRLA project lake sediment cores, " *Journal of Paleolimnology,* 3, 253-267.

Blaauw, M., and Christen, J.A. (2011), "Flexible paleoclimate age-depth models using an autoregressive gamma process," *Bayesian Analysis,* 6(3), 457-474.

Christen, J.A., and Fox, C. (2010), "A general purpose sampling algorithm for continuous distributions (the t-walk)," *Bayesian Analysis,* 5(2), 263-281.

Christen, J.A., and Pérez, S. (2009), "A new robust statistical model for radiocarbon data." *Radiocarbon*, 51(3): 1047-1059.

Gaver, D.P., and Lewis, P.A.W. (1980), "First-Order Autoregressive Gamma Sequences and Point Processes." *Advances in Advanced Probability,* Sep., 1980, Vol. 12, No. 3, pp. 727-745.

Hugus, D.H. (1982), "Extensions of some models for positive-valued time series." Ph.D. Thesis, Naval Postgraduate School, Monterey, CA.

Lewis, P.A.W., McKenzie, E., Hugus, D.K. (1989), "Gamma Processes," *Communications in Statistics. Stochastic Models,* 5:1, 1-30. DOI: 10.1080/15326348908807096.

Peck, Erin; Wheatcroft, Robert; Brophy, Laura (2019): Dataset: Controls on sediment accretion and blue carbon burial in tidal saline wetlands: Insights from the Oregon coast, U.S.A.. The Smithsonian Institution. Dataset. https://doi.org/10.25573/serc.11317820.v2

R Core Team (2019). R: A language and environment for statistical computing. R Foundation for Statistical Computing, Vienna, Austria. URL https://www.R-project.org/.

Sanchez-Cabeza, J.A. and Ruiz-Fernández, A.C. (2012), "^{210}Pb sediment radiochronology: An integrated formulation and classification of dating models," *Geochimica et Cosmochimica Acta*, 2, 183-200.

Sanchez-Cabeza, J.A., Ruiz-Fernández, A.C., Ontiveros-Cuadras, J.F., Pérez Bernal, L.H., and Olid, C. (2014), "Monte Carlo uncertainty calculation of ^{210}Pb chronologies and accumulation rates of sediments and peat bogs," *Quaternary Geochronology,* 23, 80-93.

Stan Development Team. 2018. RStan: the R interface to Stan. R package version 2.17.3. http://mc-stan.org

Appendix

Simulation Dataset

Table 1: Simulated data set using simulation set-up from Aquino-López et al. (2018)

Depth cm	$^{210}Pb(P^T)$ Bq/kg	$^{214}Pb(P^S)$ Bq/kg	σ Bq/kg	Density (ρ) g/cm^2	Depth cm	$^{210}Pb(P^T)$ Bq/kg	$^{214}Pb(P^S)$ Bq/kg	σ Bq/kg	Density (ρ) g/cm^2
1	124.821	11.560	10	1.450	16	87.296	20.785	7	1.505
2	162.234	24.180	9	1.451	17	67.811	24.387	7	1.510
3	217.550	27.809	9	1.452	18	68.030	24.346	7	1.515
4	262.580	23.445	9	1.454	19	55.102	26.754	7	1.520
5	289.136	19.031	9	1.457	20	43.459	17.049	7	1.525
6	309.120	17.581	9	1.460	21	21.588	13.002	7	1.529
7	321.573	21.160	9	1.463	22	37.582	16.731	7	1.533
8	290.653	21.266	9	1.467	23	40.010	22.930	6	1.537
9	282.283	18.812	8	1.471	24	30.032	7.968	6	1.540
10	260.445	12.473	8	1.475	25	15.575	25.286	6	1.543
11	225.055	23.455	8	1.480	26	21.845	19.710	6	1.546
12	181.015	23.210	8	1.485	27	33.004	16.709	6	1.548
13	178.695	-2.242	8	1.490	28	18.511	24.058	6	1.549
14	139.072	10.807	8	1.495	29	9.313	8.983	6	1.550
15	121.792	22.587	8	1.500	30	21.785	15.563	5	1.550